Time-resolved Morphological Study of Bulk Heterojunction Films for Efficient Organic Solar Devices

B. Paci,*,† A. Generosi,† V. Rossi Albertini,† R. Generosi,† P. Perfetti,† R. de Bettignies,‡ and C. Sentein§

Istituto di Struttura della Materia, C.N.R., Via Fosso del Cavaliere 100. 00133 Rome, Italy, Laboratoire Composants Solaires CEA INES-RDI, Savoie Technolac, BP 332, 50 Avenue du Lac Léman 73377 Le Bourget du Lac, France, and Commissariat à l'Énergie Atomique (CEA) Saclay, DRT-LITEN-DSEN-GENEC-L2C, F91191 Gif-sur-Yvette, France

Received: February 26, 2008; Revised Manuscript Received: April 11, 2008

The crucial requirement of device stability in the development of organic electronics was addressed. In particular, the nanoscale morphology of bulk heterojunction organic films for photovoltaic applications was studied by time-resolved energy dispersive X-ray reflectometry in synergy with atomic force microscopy analysis. A reorganization of the organic molecules in the film upon illumination was detected. The occurrence of two distinct processes (characterized by a reorganization of the blend bulk and an increase of its surface roughness, respectively) was revealed. Furthermore, the effect of the morphological instability on the device efficiency over time was quantified. Finally, the effect of thermal annealing treatments and of the choice of different cathodes was verified.

Introduction

An increasing amount of research activity has recently focused on organic photovoltaic (PV) cells, providing low cost conversion of solar energy. Ultrafast photoinduced electron transfer from a donor to an acceptor material provides a molecular approach to high-efficiency photovoltaic conversion[1] and is currently the basic mechanism utilized in polymer-based photovoltaic cells. Notable progress has been made in recent years using methanofullerene (acceptor) blended with poly(3-hexyl thiophene) as the donor,[2–5] reaching efficiencies exceeding 6%.[6–10] The power conversion efficiency, stability, and lifetime of such devices are the key-points to be addressed before commercial use can be considered. In particular, photovoltaic cells need to be structurally stable, both under storage conditions and upon exposure to sunlight. Under working conditions, the devices need to be resistant to both heating (due to illumination) and cooling cycles. The degradation over time of the organic film, the active component of the cell, is of particular concern in organic photovoltaic cell technology. Recently, however, it has become clear how the optical and transport properties of thin films for molecular electronics are strongly correlated to their morphology.[3,11–13] In particular, polymer regularity and film molecular packing are believed to play a crucial role, on both the optical and electrical properties of bulk heterojunction films, such as the poly(3-hexylthiophene/methano-fullerene [6,6]-phenyl C_{61} butyric acid methylester (P3HT/PCBM) blend utilized in this study. It follows that instability of the active layer morphology may be severely detrimental to the long-term efficiency of organic devices.

Here we report on the occurrence of a structural rearrangement of the active layer molecules under working conditions. The morphological bulk instability and surface roughening of the organic film were observed by in situ X-ray reflectometry and atomic force microscopy (AFM) analyses. The extent to which these processes are correlated to the deterioration of the device performances and how a preventive annealing treatment is able to stabilize the film morphology, thus enhancing the device efficiency, were also verified.

Time-resolved in situ energy dispersive X-ray reflectometry (EDXR), which has already proven itself to be a powerful tool for investigating thin films, layered samples, and devices,[14,15] is used for the first time in synergy with AFM analysis to study the structural changes of bulk heterojunction organic films for photovoltaic applications. The results indicate that the use of the two techniques, which together allow a cross monitoring of the morphological changes of a layered sample, can be successfully applied to investigate the behavior of new organic devices under real working conditions.

In the present study, the EDXR-AFM analysis focused on the morphological properties of organic P3HT/PCBM films, both under operating conditions and upon annealing. The structural changes of the blend were subsequently correlated with the performances of complete devices (which had a P3HT/PCBM film as an active component) by measuring several PV cells characterized by different metallic electrodes.

Experimental Section

Materials and Devices. Bulk heterojunction organic films were made from a blend of methano-fullerene [6,6]-phenyl C_{61} butyric acid methylester (PCBM) and poly(3-hexylthiophene) (P3HT). At present, polythiophene and its derivatives (such as P3HT) are widely studied for their semiconducting properties and, recently, for their applications in photovoltaics. The samples, fabricated following the usual procedure for PV cell construction, consisted of an indium tin oxide (ITO) substrate cleaned in an ultrasonic bath with acetone and isopropanol, then rinsed in deionized water, dried in an oven and, finally, treated with UV-ozone. The substrate is then spin-coated with a 50 nm film of poly(3,4-ethylenedioxythiophene)-poly(styrene-

* Corresponding author e-mail: Barbara.Paci@ism.cnr.it; phone: +390649934174; fax: +39064993415.
† Istituto di Struttura della Materia.
‡ Laboratoire Composants Solaires CEA INES-RDI.
§ CEA Saclay.

10.1021/jp801674v CCC: $40.75
Published on Web 06/07/2008

sulfonate) PEDOT/PSS (Baytron PH). The active layer of P3HT/PCBM was deposited by spin-casting from an anhydrous chlorobenzene solution. The first samples (sample A, B, and C) represent an intermediate step in the organic device construction; the top layer cathode was not deposited in order to have the possibility of studying the organic film surface. Subsequently, complete cells were prepared depositing different cathodes (Al, LiF/Al, and Ca/Ag) by vacuum evaporation over the active layer in order to measure their aging electrical curves.

Energy Dispersive X-ray Reflectometry Technique. X-ray reflectometry is a powerful probe to study the properties of surfaces and interfaces of layered samples, such as films deposited on substrates, multilayers, superlattices etc. This technique is based on the optical properties of X-rays, whose refraction index in a material is $n = 1 - (\lambda^2/2\pi)\rho r_0 Z^2$ (where λ is the incident wavelength, ρ is the material density, r_0 is the classical electron radius, and Z is the atomic number), although very close to 1, is not exactly unitary. As a consequence, the Snell rule still applies and, at the critical angle, it can be written as[16] $\cos\theta_c = n$. Expanding the right-hand side to the second order, we obtain $1 - \theta_c^2/2 = 1 - \rho\lambda^2 r_0 Z^2/2\pi$, which corresponds to $(\theta_c/\lambda) = Z(\rho r_0/\pi)^{1/2} =$ constant, where $\theta_c/\lambda \approx (\sin\theta_c)/\lambda \alpha q_c$ [where the critical value of scattering parameter $q_c = (4\pi \sin\theta_c)/\lambda$].

Therefore, the variable on which the reflected intensity actually depends is not the deflection angle only but, rather, the scattering parameter $q = 4\pi \sin(\theta/\lambda) = (2/hc)E \sin\vartheta$ (where E is the radiation energy, h is the Plank's constant, and c is the velocity of light). Hence, in analogy with X-ray diffraction,[17] two ways can be utilized to perform the q-scan, namely, either using a monochromatic beam and executing an angular scan [angular dispersive mode (AD)] or using a polychromatic X-ray beam at a fixed angle and carrying out an energy scan [energy dispersive mode (ED)].

Although characterized by a lower resolution with respect to the AD mode, the EDXR technique[18] benefits from the immobility of the experimental apparatus during data collection. The possibility of performing the measurements in still conditions assures that both the scattering volume of the sample and the footprint of the X-ray beam on its surface remain unchanged, which makes data analysis simpler and more reliable. Furthermore, systematic errors induced by repositioning of the diffractometer arms are prevented. Indeed, in the grazing geometry required for this kind of measurements, even minimal misallignements of the sample may induce relevant relative errors during the angular scan. In particular, if many scans have to be carried out consecutively, as in the present case, reproducibility problems that may arise because of the mechanical movements of the reflectometer arms are prevented by EDXR.

Finally, when laboratory sources (X-ray tubes) are used, the data collection is shorter in ED, because the number of photons concentrated in the monochromatic fluorescence lines (used as primary beam in AD) is much lower than the number of photons distributed along the white Bremmstrahlung component (primary beam in ED).

Of particular concern in the present study, the laboratory source used to perform the EDXR experiments produces limited X-ray fluxes (8 orders of magnitude less than in a third generation Synchrotron facility), thus ensuring that no radiation damage is induced on the organic films, despite the high energies available.

The experimental EDXR apparatus is a noncommercial reflectometer[18] characterized by a very simple setup geometry, with neither a monochromator nor a goniometer being necessary.

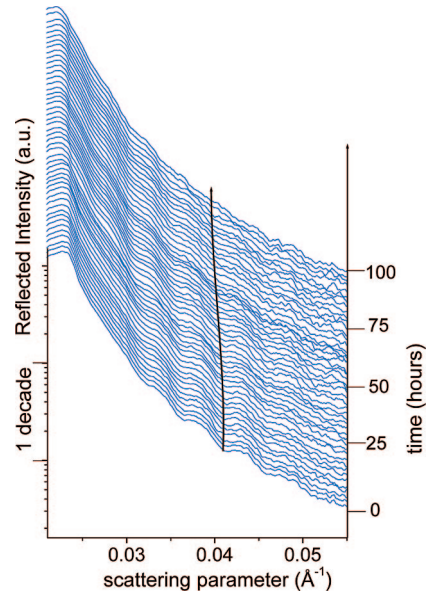

Figure 1. Time-resolved EDXR patterns collected on a P3HT/PCBM film under illumination on sample A [glass/ITO/PEDOT/(P3HT/PCBM)], over 100 h under a controlled atmosphere and upon illumination. The curves undergo a progressive compression, testified by the shift of their minima toward lower q values as a function of time (see line connecting the second oscillation minimum). This indicates an increase in film thickness, because the oscillation period Δq is connected to the film thickness (d) by the approximate relation $d = 2\pi/\Delta q$.

Indeed, because in the ED mode the scan of the reciprocal space is carried out electronically (rather than mechanically as in conventional X-ray diffraction), no movement is required during measurement. The main elements are the X-ray tube and the energy sensitive detector, both of which are mounted on two benches pivoting around a common central axis, and four adjustable slits are used to define the X-ray optical path. The bremsstrahlung of a 3 kW tungsten anode X-ray tube is used as the probe, and the energy scan is performed by an EG&G high purity germanium solid-state detector, with an energy resolution of about 1.5−2% in the 15−50 keV energy range. Each film was placed in an X-ray transparent chamber, under a controlled atmosphere of N_2 gas flux to prevent contact with external oxidizing agents, and then measured by EDXR.

Atomic Force Microscopy Analysis. The AFM measurements were performed in noncontact mode using a noncommercial air-operating atomic force microscope.[19]

Results and Discussion

A first in situ EDXR experiment consisted of collecting a sequence of X-ray reflection patterns on a glass/ITO/PEDOT/(P3HT/PCBM) multilayered system (sample A). An experimental procedure was used to maximize the P3HT/PCBM signal with respect to the one coming from the other layers. Each spectrum was acquired over a period of 1 h. The patterns were collected first in the dark (to verify that samples stored in the dark at room temperature do not show any morphological modification) and then under illumination with a white light lamp. From a qualitative point of view, the modifications of the EDXR patterns in Figure 1 can be visually interpreted by a simplified model, prior to any quantitative analysis; a variation in the period of the oscillations is related to a variation of the organic film thickness (d), and a change of the oscillation damping can be attributed to a modification of the film roughness (σ).[20]

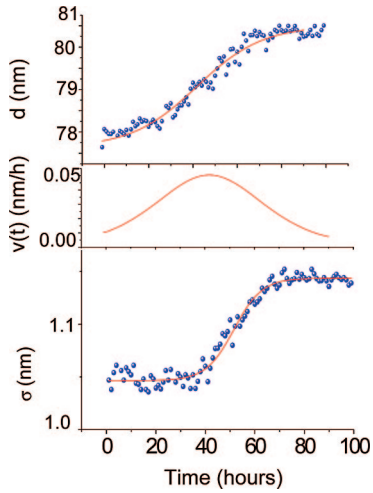

Figure 2. Morphological data points obtained as the results of data fit for sample A (film roughness σ vs time, film thickness d vs time) and film growth speed $v(t)$.

The accurate calculation of the evolution of the two morphological parameters upon illumination was obtained (see Figure 2) by analyzing the sequences of spectra according to Parratt's theory for X-ray reflectivity of stratified media.[21] The morphological data points are fitted according to two Boltzmann growth functions. The film response is not immediate (induction time of approximately 20 h). The amplitudes and time constants obtained by the fits of the data points are $\Delta d = 23 \pm 1$ Å and $\tau = 44 \pm 1$ h for the bulk process and $\Delta\sigma = 1.5 \pm 0.5$ Å and $\tau = 44 \pm 1$ h for the surface one. In the following we will show that the roughness increase is always present upon illumination, even when no change in the film thickness is observed, indicating that the roughening is essentially related to a morphological modification, rather that to the film thickness change speed $v(t)$, as shown in Figure 2. The accuracy of the time-dependent data allowed an overall variation of film roughness of only 1.5 ± 0.5 Å to be detected, close to the theoretical limit of sensitivity of the technique.

The increases in d and σ are a signature of the polymer (blend) self-organization. Indeed, a bulk reorganization of the blend will produce a modification of the film packing, detectable as a change in its morphological parameters.

This hypothesis was confirmed by the AFM maps (see Figure 3, panels a and b) collected on the same sample (sample A) measured by in situ EDXR. These AFM images show the surface state of the above sample before and after illumination. The effect of the illumination on the surface of the organic layer is remarkable; the polymers, initially homogenously dispersed in the matrix (200 nm width and 20 nm high domains), had become structurally organized during illumination, with an enhanced crystalline order along a preferential orientation being evident in Figure 3b. Nevertheless, no direct evidence of demixing of the two components was found within the range of temperature and time utilized in this study. This structural modification is probably due to a thermal effect, because the illuminated sample reaches about 70 °C, that is, a temperature close to the P3HT glass transition temperature.

To verify this hypothesis, further investigations were performed on a new sample of the same structure [glass/ ITO/ PEDOT/(P3HT/PCBM), sample B]; the organic film was first analyzed by AFM, was subsequently measured by in situ EDXR in the dark and upon heating at $T = 70$ °C for 150 h (Figure 4), and measured again by AFM (Figure 3c). The EDXR results show that the blend undergoes a structural modification, similar to that observed in the previous case, characterized by a monotonic increase of the film thickness. It must be specified that the thickness and roughness of the various samples, although similar, can vary from sample to sample, because the deposition method induces statistical fluctuations on the initial morphological parameters. The comparison of the AFM measurements, performed before and after sample heating, confirms that the process observed by EDXR is consistent with a self-organization of the blend. Indeed, the surface morphology of the film "as deposited" is qualitatively analogous to that of sample A (therefore, it is not reported in Figure 3), that is, the polymers are initially homogenously dispersed in the blend matrix. During heating, the organic film of sample B becomes structurally organized, as shown in Figure 3c, and its final morphology is qualitatively analogous to that of sample A after illumination. In particular, the AFM results indicate that the final (post annealing/post illumination) morphology of the two samples is characterized by oriented and ordered crystalline structures of analogus dimension (see also the line profiles in Figure 3).

We can conclude that the morphological change underwent by the organic film of sample A was induced by sample heating, caused by illumination. Indeed, the same phenomenon is observed even in the dark, by reproducing the thermal conditions of a working device (sample B), with the process being faster in the latter case. Therefore, the morphological modifications observed for the pristine samples, involving the active layers structural self-organization and accompanied by an increase of the surface roughness, appear unavoidable unless cooling of the operating device is performed, which may not be convenient.

At this point, the main question to be addressed regards the consequence of the observed (surface and bulk) structural instability of the active layer on the organic device performances.

We can safely predict the consequence of the surface deterioration; the increase observed in the active layer roughness should worsen the contact between the organic film and the metallic electrode in a complete cell, leading to a lower photocurrent.

The effect of the film bulk self-organization is, on the contrary, not as easy to predict, because competing processes are expected. Indeed, a high polymer regularity of the blend may enhance the hole mobility, improving the device's performance, as the size of the domains is crucial to charge carrier transport. Conversely, a possible phase segregation into large PCBM clusters separated by P3HT crystals (of micrometric size) may be detrimental. To obtain efficient dissociation of excitons inside the bulk heterojunction, the donor and the acceptor molecules should form an interpenetrated network at the nanometer scale to maximize the interface area.

Therefore, to quantify the aging consequences of the observed morphological changes and to verify whether it is possible to inhibit or limit the device deterioration, we investigated, using the same method applied above, the result of preventive thermal annealing treatments on the organic film stability.

A new sample of the same structure [glass/ITO/PEDOT/(P3HT/PCBM), sample C] was deposited and pretreated by thermal annealing (110 °C for 30 min) in situ before being measured by EDXR, initially in the dark and than upon illumination for 150 h. AFM images (Figure 3, panels d−f) were acquired on the sample as deposited, after annealing and after illumination. The results of the EDXR data analysis reported in Figure 5 confirm the stability of the morphological parameter when the sample is stored in the dark, as evidenced by the data points before time zero (time zero being the instant in which

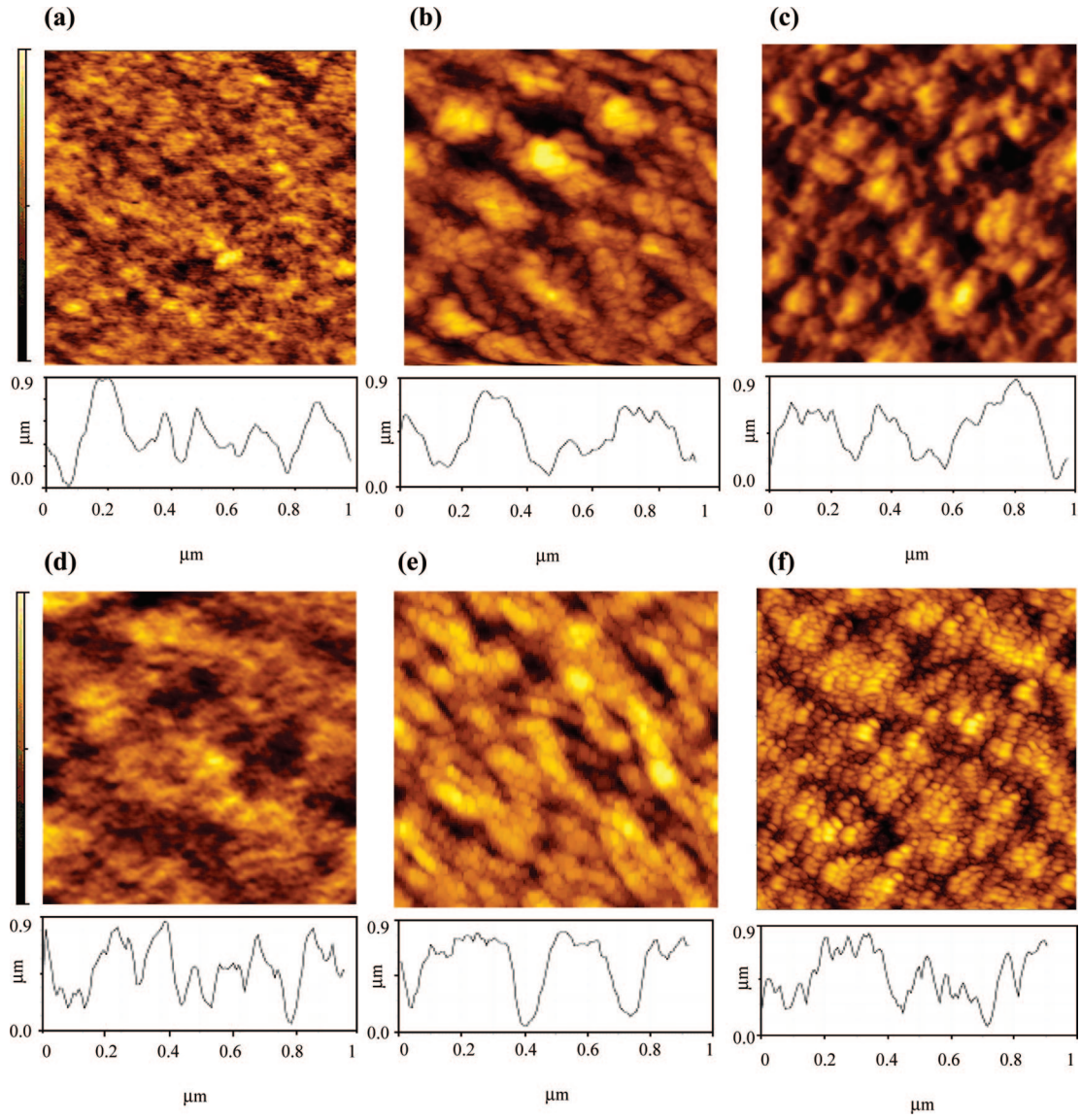

Figure 3. AFM images of P3HT/PCBM films and line profiles. (a) AFM images acquired on sample A as deposited. (b) AFM images acquired on sample A after illumination. (c) AFM images acquired on sample B after heating at T= 70 °C for 150 h. (d) AFM images acquired on sample C as deposited. (e) AFM images acquired on sample C after annealing at 110 °C for 30 min. (f) AFM images acquired on sample C after annealing and illumination for 150 h. A thinner structure is also visible in panel f due to the extremely high resolution obtained. All samples have the same structure: glass/ITO/PEDOT/(P3HT/PCB).

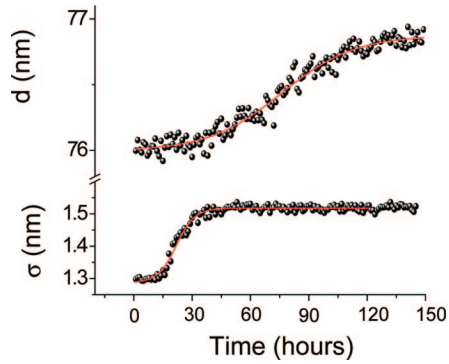

Figure 4. Time evolution of the morphological parameter obtained from in situ EDXR measurements (collected under a controlled atmosphere, keeping the sample in the dark, and upon heating at T= 70 °C) for a pristine cell (sample B). Film thickness *d* vs time and film roughness σ vs time curves.

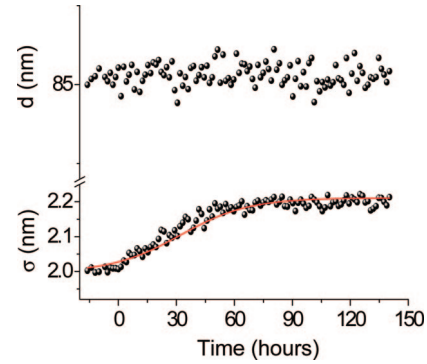

Figure 5. Morphological data points (film roughness σ vs time, film thickness *d* vs time) of a preannealed P3HT/PCBM film (sample C), obtained by time-resolved EDXR measurements upon illumination.

the light is turned on). Moreover, these results show that the sample thickness is stable upon illumination whereas the roughness increases, demonstrating that heating always influences the film roughness, even when no effect on its thickness is produced. This stability of the film thickness suggests that the preventive annealing process is able to limit the modification

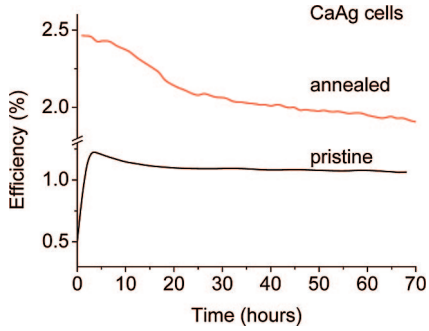

Figure 6. Annealing effect on the aging curves of glass/ITO/PEDOT/(P3HT/PCBM)/Ca/Ag cells. Comparison of the aging curves of a pristine cell and an annealed cell using a Ca/Ag cathode. Pre-annealing at 110 °C.

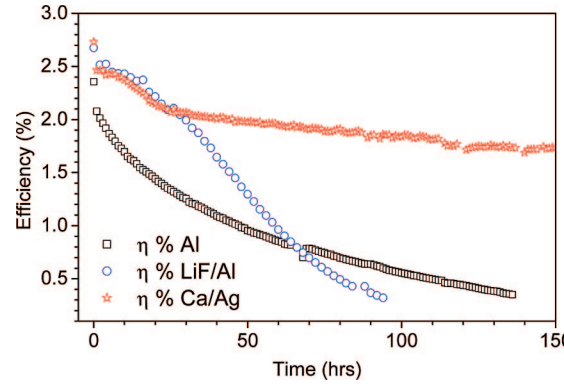

Figure 7. Aging curves of P3HT/PCBM based cells as a function of the cathode used. Aging curves of PV cells having different metallic cathodes based on P3HT/PCBM films under AM 1.5 illumination, 100 mW/cm^2. The structures of the cells are glass/ITO/PEDOT/(P3HT/PCBM)/Al, glass/ITO/PEDOT/(P3HT/PCBM)/LiF/Al, and glass/ITO/PEDOT/(P3HT/PCBM)/Ca/Ag.

of the bulk structure of the active layer. This is confirmed by the AFM data; Figure 3d shows that the surface morphology of the pristine film is the same as the other two films (polymers are initially homogenously dispersed in the blend matrix). The preventive thermal annealing produced a self-organization of the film. Of particular note is the fact that the image of the annealed film (Figure 3e) is analogous to those of the illuminated and heated films reported above (Figure 3, panels b and c). Finally, the last AFM map shows that the morphology recorded after illumination (Figure 3f) is still characterized by a similar morphology, although a thinner structure is also visible due to the extremely high resolution obtained. These data, together with the film thickness stability obtained by EDXR, suggest that the annealed sample did not undergo a significant structural change upon illumination.

We can therefore state that a preventive annealing process (at 110 °C) is able to limit the modification of the bulk structure of the active layer, producing a self-organization process of the polymer that may be controlled a priori. In turn, the observed nanoscale morphological order results in a large increase in efficiency of the annealed cell. This increase in efficiency is evident by comparing the aging curves under simulated AM 1.5 100 mW/cm^2 illumination of two new samples, that is, a pristine and an annealed cell as reported in Figure 6 (cell structures are glass/ITO/PEDOT/(P3HT/PCBM)/CaAg and annealing was performed at 110 °C for 30 min).

On the other hand, a roughening of the organic film layer surface takes place upon illumination, even in the case of the annealed sample (sample C, Figure 5). This morphological instability compromises the contact between the active layer and the metallic electrode when the cell is working, causing a decrease in the cell efficiency over time. The organic layer−electrode interface contribution to the overall cell aging is evident in the case of the annealed cell (see aging curve in Figure 6), where no bulk phenomenon occurs. Therefore, we can state that the annealing procedure stabilizes the bulk morphology of the organic film and thus raises the initial efficiency; however, it is not able to prevent the aging of the device, because a deterioration of the organic film−electrode contact persists. In the case of pristine cells this negative effect is less evident, and the efficiency decreases more slowly. This is probably due to the fact that the interface deterioration may be compensated by the bulk reorganization of the blend that might lead to an improvement of the cell photocurrent.

As a more general statement we may say that, when a complete device is studied, the stability of the organic layer−electrode interface is a crucial parameter to take under control. It follows that a key point to address is whether the degradation of the metallic electrode buried interface may be decreased by an appropriate cathode choice. For this reason, the present study was concluded by a comparative investigation of several cells varying in metallic electrodes. The devices were submitted to a preventive annealing treatment, to stabilize their bulk structure (as discussed), so that only a roughening of the organic film−metallic electrode interface was expected. The aging curves reported in Figure 7 confirm that the expected deterioration of the polymer−electrode interface is still present, as all devices show a loss in their efficiency over 60 h of working.

Nevertheless, the shapes of the curves demonstrate that this effect depends on the type of electrode; the effect is most evident in the case of the Al electrode and is minimal in the case of the Ca/Ag electrode. In the case of the device having the Al electrode in direct contact with the blend, the loss in efficiency appears to be much faster in the first part of the curve with respect to the other two cells, in accordance with the literature reporting on the critical instability observed in working plastic PV cells at the aluminum electrode−organic film interface.[1415]

Conclusions

The experimental results directly correlate the real-time structural evolution of the active layer of a working organic PV cell to the deterioration of the device performances. This was obtained by applying the time-resolved EDXR technique in situ (in order to provide the morphological variations of the organic film under operating conditions) in combination with AFM measurements. The new approach used in this work allowed the direct detection of a reorganization of the organic molecules in the film. We revealed the occurrence of two distinct processes (namely a reorganization of the blend bulk and an increase of its surface roughness) and quantified their effect on the device efficiency over time. Furthermore, we demonstrated that the former can be inhibited by thermal annealing treatments capable of stabilizing the organic layer bulk morphology. Finally, the present study demonstrates that the effect of the degradation of the metallic electrode buried interface may be strongly reduced by an appropriate choice of the cathode. The information obtained uncovers some uncontrolled mechanisms limiting the cell efficiency, stability, and lifetime, and may be used for further improvements in organic electronics.

References and Notes

(1) Sariciftci, N. S.; Smilowitz, L.; Heeger, A. J.; Wudl, F. *Science* **1992**, *258*, 1474.

(2) Brabec, C. J. *Sol. Energy Mater. Sol. Cells* **2004**, *83*, 273.
(3) Yang, X. N.; Loos, J.; Veenstra, S. C.; Verhees, W. J. H.; Wienk, M. M.; Kroon, J. M.; Michels, M. A. J.; Janssen, R. A. J. *Nano Lett.* **2005**, *5*, 579.
(4) Krebs, F. C.; Spanggaard, H. *Chem. Mater.* **2005**, *17*, 5235.
(5) de Bettignies, R.; Leroy, J.; Firon, M.; Sentein, C. *Synth. Met.* **2006**, *156*, 510.
(6) Li, G.; Shrotriya, V.; Huang, J. S.; Yao, Y.; Moriarty, T.; Emery, K.; Yang, Y. *Nat. Mater.* **2005**, *4* (11), 864.
(7) Kim, Y.; Cook, S.; Tuladhar, S. M.; Choulis, S. A.; Nelson, J.; Durrant, J. R.; Bradley, D. D. C.; Giles, M.; Mcculloch, I.; Ha, C. S.; Ree, M. *Nat. Mater.* **2006**, *5* (3), 197.
(8) Peet, J.; Kim, J. Y.; Coates, N. E.; Ma, W. L.; Moses, D.; Heeger, A. J.; Bazan, G. C. *Nat. Mater.* **2007**, *15* (10), 1617.
(9) Kim, K.; Liu, J.; Namboothiry, M. A. G.; Caroll, D. L. *Appl. Phys. Lett.* **2007**, *90*, 163511.
(10) Ma, W.; Yang, C.; Gong, X.; Lee, K.; Heeger, A. J. *Adv. Funct. Mater.* **2005**, *15* (10), 1617.
(11) Yang, X. N.; van Duren, J. K. J.; Janssen, R. A. J.;; Michels, M. A.; Loos, J. *Macromolecules* **2004**, *37*, 2151.
(12) Erb, T.; Zhokhavets, U.; Gobsch, G.; Refiya, S.; Stühn, B.; Schilinsky, P.; Waldauf, C.; Brabec, C. J. *Adv. Funct. Mater.* **2005**, *15*, 1193.
(13) Sevenije, T. J.; Kroeze, J. E.; Yang, X.; Loos, J. *Adv. Funct. Mater.* **2005**, *15*, 1260.
(14) Paci, B.; Generosi, A.; Rossi Albertini, V.; Perfetti, P.; de Bettignies, R.; Firon, M.; Leroy, J.; Sentein, C. *Appl. Phys. Lett.* **2006**, *89*, 043507.
(15) Paci, B.; Generosi, A.; Rossi Albertini, V.; Perfetti, P.; de Bettignies, R.; Firon, M.; Leroy, J.; Sentein, C. *Appl. Phys. Lett.* **2005**, *87*, 194110.
(16) James, R. W. *The Optical Principles of the Diffraction of X-ray*; OX BOW Press: Woodbridge, CT, 1982.
(17) Caminiti, R.; Rossi Albertini, V. *Int. Rew. Phys. Chem.* **1999**, *18* (2), 263.
(18) Rossi Albertini, V.; Paci, B.; Generosi, A. *J. Phys. D* **2006**, *39*, 461.
(19) Cricenti, A.; Generosi, R. *Rev. Sci. Instrum.* **1995**, *66* (4), 2843.
(20) Sinha, S. K.; Sirota, E. B.; Garoff, S.; Stanley, H. B. *Phys. Rev. B* **1988**, *38*, 2297.
(21) Parratt, L. G. *Phys. Rev.* **1954**, *95*, 359.

JP801674V